

Carbon Materials as Anode for Lithium Ion Batteries: Materials and Design Aspects

M.Suresh
(CH14MTECH11007)

A Dissertation Submitted to
Indian Institute of Technology Hyderabad
In Partial Fulfillment of the Requirements for
The Degree of Master of Technology

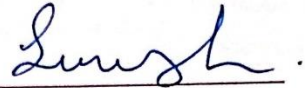


Department of Chemical Engineering

June, 2016

Declaration

I declare that this written submission represents my ideas in my words, and where others' ideas or words have been included, I have adequately cited and referenced the original sources. I also declare that I have adhered to all principles of academic honesty and integrity and have not misrepresented or fabricated or falsified any idea/data/fact/source in my submission. I understand that any violation of the above will be a cause for disciplinary action by the Institute and can also evoke penal action from the sources that have thus not been properly cited, or from whom proper permission has not been taken when needed.



(Signature)

M. Suresh

(Student Name)

CH14MTECH11007

(Roll number)

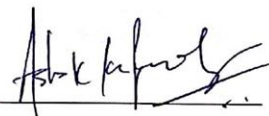
Approval Sheet

This thesis entitled “Carbon Materials as Anode Materials for Lithium Ion Batteries: Materials and Design Aspects” by M. Suresh is approved for the degree of Master of Technology from IIT Hyderabad.



Dr Saptarshi Majumdar
IIT Hyderabad
Examiner

Dr Debaprasad Shee
IIT Hyderabad
Examiner



Dr Ashok Kumar Pandey
IIT Hyderabad
Examiner



Dr Chandra Shekhar Sharma
IIT Hyderabad
Adviser

Acknowledgements

I express my sincere gratitude to my Supervisor **Dr Chandra Shekhar Sharma** for his patient guidance and constant encouragement throughout my project. I am fortunate to have a guide like him. I would like to express my heartfelt thanks for his excellent guidance.

I would like to thank my committee members **Dr(s). Saptarishi Majumdar, Debaprasad Shee** and **Ashok Pandey** for their valuable inputs.

I would like to thank my colleagues **Dr Manohar Kakunuri, Mr Srinadh, Mrs Ramya** and **Mr Karthik M.G.** for helping me with my experiments and training in various equipment.

I would also like to thank my colleagues, **Kali Suresh, Aninditha, Utkarsh, Anand, Radha, Krishna**, and for helping me with various characterization.

I would also like to thank my friends who have supported me a lot to get rid of my stress.

I would like to thank my other lab mates **Akash, Aditya, Shubham, Sanjana, Pujitha**, for their support and encouragement.

Lots of love to my **Parents** for their unconditional love and their selflessness sacrifices for putting me in a comfort zone.

Abstract

In this thesis work, Carbon based anode materials have been investigated, and we reported how microstructure changes affect the electrochemical performance when used as an anode for Lithium-Ion batteries. We have explored two hard carbon precursors: Polyvinylidene fluoride (PVDF) polymer and SU 8 (epoxy based resin). Depending upon the precursors and synthesis conditions hard carbons differ in their microstructure regarding crystallinity, porosity, morphology and also in the heteroatoms content and functional groups. To enhance the electrochemical performance we have optimized different synthesis parameters like pyrolysis temperature for PVDF and varied the aspect ratios in case of SU 8. We used different characterization techniques like Brunauer-Emmett-Teller, Transmission Electron Microscopy, Scanning Electron Microscopy, X-ray diffraction, 3D Optical Profiler and Fourier Transform Infrared Spectroscopy to determine their microstructure, crystallinity and functional groups attached. We performed Galvanostatic charge/discharge experiments and cyclic voltammetry to determine the electrochemical performance.

We reported the electrochemical performance of Polyvinylidene fluoride (PVDF) derived carbon obtained at different pyrolysis temperatures. This material shows reversible capacity (478 mAh/gm), which is significantly higher than the theoretical capacity of graphite (372 mAh/gm). We also improved the yield of carbon from the polymer by adding dehydrofluorination step. We believe that functional groups present in carbon obtained at low temperatures play a significant role in the electrochemical performance of the cell. Hence, we used FTIR to detect the changes in functional groups and correlated the changes with electrochemical performance and got the best performance at 1400°C in minimal presence of Fluorine functional groups.

Typically, Lithium ion battery electrodes are of thin layer coated on a conductive foil with limited surface area, to have more surface area to enhance Li-ion intercalation we fabricated carbon based 3D microelectrodes on SS wafers. SU 8 is one the most well-known epoxy-based negative tone photoresists which we have chosen as a carbon precursor. We have successfully fabricated the stable SU 8 micropillars with

different aspect ratios on SS wafer for the first time and derived micro carbon structures upon pyrolysis.

Using 3D optical profiler we determined the aspect ratios of the structures. We have reported the electrochemical performance of the carbon microelectrode but still we found that there is a need to increase the aspect ratio and density of micron size structures for better electrochemical performance.

Nomenclature

| | |
|----------|--|
| CDA-900 | Carbon derived from PDA at 900°C |
| CDI-1200 | Carbon derived from PDI at 1200°C |
| CDI-900 | Carbon derived from PDI at 900°C |
| FESEM | Field Emission Scanning Electron Microscope |
| HRTEM | High Resolution Transmission Electron Microscope |
| PDA | PVDF dehydrofluorinated in air |
| PDI | PVDF dehydrofluorinated in inert atmosphere |
| PVDF | Polyvinylidene fluoride |
| SEI | Solid Electrolyte Interphase |
| XRD | X-ray Diffraction |

List of Tables

| | | |
|------------------|--|-----------|
| TABLE I | Summary of specific capacities of CDI samples pyrolyzed at different temperatures at 0.1 C- rate | 11 |
| TABLE II | Summary of yields of carbon at different Temperatures | 12 |
| TABLE III | Summary of micropillars fabricated with different Aspect ratios | 18 |

List of Figures

| | | |
|------------------|--|-----------|
| Figure 1 | Schematic of a lithium ion battery | 1 |
| Figure 2 | FESEM images of a) PVDF Powder & b) CDI-1400; | 7 |
| Figure 3 | HRTEM images of CDI-1400 at different magnifications | 8 |
| Figure 4 | Comparison of FTIR spectrum of a) PVDF; b) PDI; c) CDI-900; d) CDI-1400 | 9 |
| Figure 5 | XRD plots of carbon derived at different temperatures a) CDI 900; b) CDI 1200 and c) CDI 1400 | 10 |
| Figure 6 | Comparison of C-rate capability of a) CDI -900 ,CDI -1200 and CDI -1400. | 11 |
| Figure 7 | Cyclic voltammetry study a) CDI 900; b) CDI 1200; c) CDI 1400 | 13 |
| Figure 8 | Schematic of C-MEMS | 22 |
| Figure 9 | Schematic of Fabrication process of 514 micron height pillars | 17 |
| Figure 10 | SEM images of SU 8 derived carbon micropillars | 18 |
| Figure 11 | 3D image of SU 8 micropillars of sample 220 microns height | 26 |

| | | |
|------------------|---|-----------|
| Figure 12 | 2D image of SU 8 micropillars of 220 micron height | 19 |
| Figure 13 | 3D image of SU 8 derived carbon micropillars | 20 |
| Figure 14 | 2D image of SU 8 derived carbon micropillars | 20 |
| Figure 15 | Galvanostatic Charge/Discharge of microelectrode at 0.1C Rate | 21 |

Scientific Contributions from This Work

Manuscripts (Under Preparation):

- Mamidi Suresh; K. M. Gopala Krishna; Chandra S. Sharma; “PVDF Derived Carbon as Anode for Lithium Ion Batteries”, *ECS Transactions*.
- M. Kakunuri ; Mamidi Suresh ; C. S. Sharma “ SU-8 Photoresist Derived 3D Carbon Microelectrode As High Capacity Anode Material for Lithium Ion Battery”, *ECS Transactions*.

Table of Contents

| | |
|--|----------|
| Declaration | i |
| Approval Sheet | ii |
| Acknowledgements | iii |
| Abstract | iv |
| Nomenclature | vi |
| List of Tables | vii |
| List of Figures | viii |
| | |
| 1. Introduction | 1 |
| 1.1 Introduction to lithium ion battery | 1 |
| 1.1.1 Working mechanism of Li-ion battery | 1 |
| 1.1.2 Carbon as anode materials for lithium ion battery | 2 |
| 1.2 Objectives | 4 |
| 1.3 Layout of the thesis | 4 |
| | |
| 2. PVDF derived carbon as Anode for Lithium Ion Batteries | 5 |
| | |
| 2.1 Introduction | 5 |
| 2.2 Materials and methods. | 6 |
| 2.2.1 Preparation of PVDF solution | 7 |
| 2.2.2 Dehydrofluorination of PVDF | 7 |
| 2.2.3 Pyrolysis at different Temperatures | 7 |
| 2.2.4 Electrode preparation | 7 |
| 2.3 Characterization | 7 |
| 2.3.1 FESEM characterization | 7 |
| 2.3.2 HRTEM characterization | 8 |
| 2.3.3 FTIR Characterization | 8 |
| 2.3.4 Characterization by XRD | 9 |
| 2.4 Electrochemical Performance of CDI X Samples | 10 |
| 2.4.1 Galvanostatic charge/discharge cycling at 0.1 C Rate | 11 |
| 2.4.2 Cyclic voltammetry | 13 |
| 2.5 Conclusions | 14 |

| | |
|---|-----------|
| 3. 3D Carbon Fractal Structures as Anode for Lithium Ion Battery | 15 |
| 3.1 Introduction | 15 |
| 3.2 Materials and methods | 16 |
| 3.2.1 Fabrication of different aspect ratios | 17 |
| 3.2.2 Pyrolysis | 18 |
| 3.2.3 Electrode preparation | 18 |
| 3.3 Characterization | 18 |
| 3.3.1 SEM characterization | 18 |
| 3.3.2 Optical Profiler analysis | 20 |
| 3.4 Electrochemical performance of different aspect ratio samples | 21 |
| 3.4.1 Galvanostatic charge/discharge cycling at 0.1 C Rate | 21 |
| 3.5 Conclusions | 22 |
| 4. Summary and Future Directions | 23 |
| 4.1 Summary | 23 |
| 4.1.1 Fine tuning of hard carbon | 23 |
| 4.1.2 Characterization | 24 |
| 4.1.3 Electrochemical performance | 24 |
| 4.2 Future directions | 24 |
| References | 26 |

Chapter 1

Introduction

1.1 Introduction to lithium ion battery

A battery is a device which converts chemical energy into electrical energy. It consists of an anode, cathode, separator and electrolyte. Based on their charge discharge mechanism batteries are classified into two types i.e. primary and secondary. Primary batteries are non-rechargeable while secondary batteries are rechargeable.

Li-ion battery is the commercially used secondary battery powering laptops, mobiles and now being explored for electric vehicles as well. The term Li-ion is used because of the unique principle of intercalation of Li ions into the host like structures of electrodes. The Li-ions can reversibly intercalate and de-intercalate thus enabling charging and discharging of the battery. Initially, in 1970's Li-ion batteries were introduced, Li metal was used as anode material, but its usage is impaired because of its safety concerns like dendrite formation, which leads to short circuits [1]. In the 1990s, Sony first introduced the Lithium-ion battery into the market which has then since become indispensable where they replaced anode material with carbon which shows excellent cyclic behaviour. Li-ion batteries dominate the other rechargeable batteries because of its high power and energy densities with small self-discharge.

1.1.1 Working mechanism of Li-ion battery:

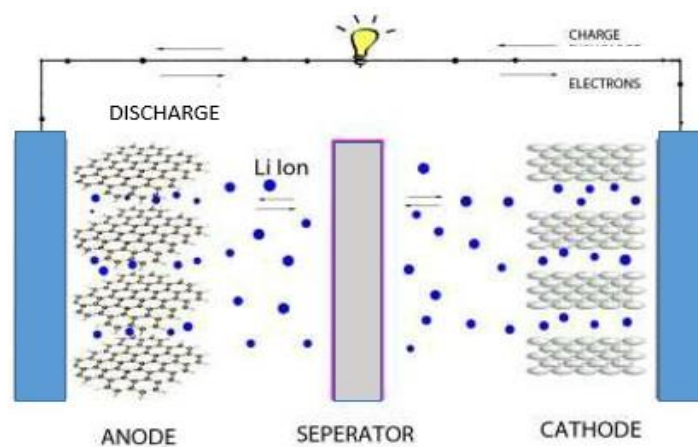


Figure 1: Schematic of a lithium ion battery

A Li-ion battery mainly consists of an anode, cathode, electrolyte and a separator. These electrodes can accommodate the ionic form of lithium. A separator which is a porous membrane separates these electrodes. The electrode active materials were coated on a conductive substrate which acts as current collectors. A lithium salt dissolved in organic carbonate solution is used as the electrolyte. Initially, there will be no migration of Li ions, upon applying an external voltage i.e. negative potential to an anode and positive to a cathode, to balance the charge Li ions migrate from cathode to anode through ionically conductive electrolyte. So upon discharging spontaneously, Li ions move towards cathode giving electrons to an external circuit. The process of Li ions insertion in carbon material during charging is named as intercalation and process of removal termed as de-intercalation. Six carbon atoms accommodate one Li ion on average in graphite anode.

During the first cycle, The Li ions react spontaneously with the electrolyte on the surface of carbon and forms a passive layer called solid electrolyte interphase (SEI).The SEI layer comprises of Lithium Alkyl Carbonates, Sulphides, oxides, and halides [2]. This reaction which consumes Li ions is irreversible so there will be a loss of capacity in Initial cycles termed as an Irreversible capacity. In the absence of this layer, Li ions co-intercalate with electrolyte molecules and exfoliates the graphite. So the safety depends on how fast this layer forms before co-intercalation happens. This SEI layer secures electrode by preventing it from further reacting with the electrolyte at higher negative voltage [2].

1.1.2 Carbon as anode materials for lithium ion battery

Carbon is the basic building block of life. The carbonaceous materials have been adopted in many electrochemical energy storage systems. Sony Corp. Ltd. developed the Li-ion battery first time in 1991 with carbon as the anode. Carbon was preferred as the anode material because of its excellent conductivity, lower redox potential, low charge-transfer resistance at the interface between the electrolyte. Carbon is a unique element which exists in different allotropic forms like graphite, diamond, amorphous carbon, Q-Carbon and now with Nanostructuring new allotropes like nanofibers, nanotubes, buckyballs and graphene also been synthesised.

Carbonaceous materials are classified into two categories based on their crystallinity graphitic and non-graphitic (disordered) based on their structures [3].

Graphite is made up of stacked graphene layers which are highly oriented in the hexagonal crystal structure. Non-graphitic carbons are divided into two types, i.e., soft carbon and hard carbon based their crystallite sizes. Graphite is widely used anode material in Li-ion battery. Though it is theoretically limited to 372mAh/g, it is still used because it is easily available and inexpensive. Graphene has carbon in sp² hybridization with one free electron in the valence band, so it acts as a good conductor as well. Intercalation of one lithium requires six carbon atoms and primarily Li-ion storage is possible only due to intercalation mechanism. The advantage of graphite is its flat discharge voltage profile due to which current need not compensate for the loss in voltage and thus offers constant voltage during discharge [4].

Soft carbons are one of the non-graphitizing carbons which have small crystallites arranged uniformly in a very short range order. When we heat this soft carbons at high temperatures (~2000°C), on cooling they align and thus gets graphitized. Soft carbons give higher specific capacity because of insertion mechanisms operating in addition to intercalation mechanism. Li-ions may get inserted into nanopores due to disorientations of Graphene layers. The disadvantage is that they have low density, large irreversible capacity and poor cyclability [5].

Hard carbons have tiny crystallites where graphene layers are highly disoriented, arranged like a house of cards [6]. They possess a lot of structural disorders and it is difficult to graphitize them even at higher temperatures (~ 3000 ° C). The main advantage with this hard carbon is high specific capacity, here the high capacity is due to the Li-insertion in micropores and mesopores formed due to the disorientation of graphene layers. It has disadvantages like High Irreversible capacity, low density and capacity degradation at higher current densities [5].

There are numerous reports on organic precursors which yield Hard Carbon. Depending on the precursor and temperature, hard carbons vary in microstructure like crystallinity, morphology, porosity and functional groups. The structural parameters play a major role in optimizing the electrochemical performances. The morphology of a fractal or interconnected structure helps in the facile diffusion of Li-ions [7]. The movement of Li-ions is also affected by the density of the particles which in turn depends on porosity [8]. The presence of foreign atoms [9] and functional groups [10] also affect the capacity. These Functional groups react with Li ions irreversibly and leads to capacity fade. Thus, a careful selection of precursors and pyrolysis program helps in developing high capacity hard carbon anodes.

1.2 Objectives

The main objective of the work is to understand how different synthesis condition help us to optimize the performance of hard carbons.

To fabricate 3D carbon microelectrodes as anode material so that we can have more accessible surface area and short diffusion length for Li ions when compared to thin film based anode material.

1.3 Layout of the thesis

Thesis first begins with a brief introduction to lithium ion battery mechanism before focusing on different carbon materials that are used as an anode for lithium ion battery.

In chapter 2, we chose PVDF as a precursor for hard carbon and studied the changes in surface functional groups and crystallinity with temperature. We have also studied their effects on electrochemistry.

In chapter 3, we used SU 8 as a precursor for hard carbon with stainless steel as substrate and studied the affected change in aspect ratio on electrochemistry.

Finally in chapter 4, we summarize the major findings of this work and discuss the future directions.

Chapter 2

PVDF derived Carbon as Anode for Lithium Ion Battery

2.1 Introduction

Li-ion batteries are predominantly used as rechargeable batteries. It gained attention for applications as high energy density power sources. The problem of dendrite formation [11] in Li metal batteries was overcome by replacing Li metal as an anode by carbon materials. They can store Li ions reversibly. Sony became the first company which commercialised the Li-ion batteries. As a matter of fact, many carbon materials have been reported since last two decades from highly oriented pyrolytic graphitic carbons to disorder hard carbons. However, to our knowledge the graphitic carbon as anode material in Li-ion batteries is widely available on the market because of its ability to have good cyclability and stable cyclic performance. Because of its low specific capacity (theoretical limit $\sim 372\text{mAh/g}$), there was a necessity to search for an alternative to meet demands of high capacity applications [12]. Recently there have been numerous reports on preparing high capacity carbons which are obtained by pyrolysis of various organic precursors (PVC, Pitchblende etc.) for Li-ion battery application [13].

PVDF (Polyvinylidene fluoride) is fluoropolymer which consists of vinylidene fluoride as a monomer. It is well known as a binder material in electrode preparation which acts as a binder between carbon active material and the current collector. T Zheng et. al. [15] proposed that PVDF can be blended with various polymers used as gel based polymer electrolytes. T. Zheng et. al. [13] reported PVDF as an organic precursor for carbon which was pyrolyzed at different temperatures (below 1000°C), but the yield so obtained was low ($\leq 20\%$). At the same time, they reported only 1st cycle capacity. Kise [14] et al. investigated the removal of fluorine from PVDF partially in an aqueous medium with ammonium salts.

In our present work, we studied the capacity dependence on pyrolysis temperature and observed how structural changes lead to the improvement of capacity. We also report a high yield of carbon by adding dehydrofluorination step before pyrolysis (~70%) which is significantly higher than reported value in T Zheng et. al. [15].

2.2 Materials and Methods

Materials:

Sodium Hydroxide (97% purity), LP-30 electrolyte (1 M LiPF₆ in 1:1 v/v mixture of ethylene carbonate and diethyl carbonate) were procured from Merck, India. Lithium foil (99.9% trace metal basis) and Poly (vinylidene fluoride) (PVDF) (99.9% purity), was obtained from Sigma-Aldrich, India. Tetra-n-butyl ammonium bromide (TBAB) (98% purity) was purchased from Alfa Aesar, India. We used stainless steel (SS) foil (polycrystalline SS 316, 100 μm thick) as a current collector and procured the same from MTI corp., USA. Deionized water was used as a solvent for preparing sodium hydroxide solution. All chemicals were used directly without any further modifications.

2.2.1 Dehydrofluorination:

1 gm. of PVDF powder was added to 40 ml solution containing 4M NaOH and 12.5mM TBAB under inert atmosphere inside a glove box. The solution was kept under constant stirring for 2 hours at 70° C. The solution turns black in colour which indicates the onset of reaction. After the reaction, the aqueous phase is separated from polymer phase by filtration followed by washing with ethanol and methanol. The polymer phase was then oven dried at 70° C for 12 hours [15]. The samples which were dehydrofluorinated in an inert atmosphere was labelled as PDI.

2.2.2 Pyrolysis of dehydrofluorinated PVDF:

The dehydrofluorinated powder was pyrolyzed in a tubular furnace (Nabertherm, Germany). After introducing the sample into the furnace tube, the tube was purged with nitrogen gas. After purging the chamber, nitrogen gas flow was maintained throughout the pyrolysis process at the rate of 50 l/hr. The ramp rate which was used to get the desired temperature is 5°C/min and then dwelled at the same temperature for 1 hour. The sample was then cooled to room temperature in the presence of nitrogen. Carbon obtained by pyrolysis of

PDI was labelled as CDI-X. The X is used to denote the pyrolysis temperature. After pyrolysis of each sample, names were given as CDI-900, CDI-1200, and CDI-1400 for samples pyrolyzed at 900, 1200 and 1400.

2.2.3 Electrode Preparation:

For electrochemical studies, SS foil was used as the current collector. The slurry was prepared by dissolving 10% Polyvinylidene fluoride (PVDF) and 90% CDI-X in N-Methyl-2-pyrrolidone (NMP) solvent. The working electrode was prepared by coating this slurry on SS foil followed by vacuum drying at 120°C. The Lithium foil serves as a counter electrode. Glass microfiber filter (Whatman, Grade GF/D) soaked in LP-30 electrolyte was used as a separator between two electrodes and packed inside the argon filled glove box using Swagelok cell assembly. Before electrochemical testing, the electrochemical cells were soaked for 12 h. Potentiostat/ Galvanostat (Bio-Logic Science Instruments, Model VSP) was used to study the electrochemical performance of packed half-cells.

2.3 Characterization:

Field Emission Scanning Electron Microscope (FESEM, SUPRA 40 Zeiss) and high-resolution transmission electron microscopy (HRTEM) (FEI Tecnai G2S-Twin) were used to study the morphological changes in structure. Powder X-ray measurements were recorded in scattering angle range of 10° to 60° on PANalytical X-ray diffractometer with CuK α radiation to study the crystallinity of the sample. Fourier Transform Infrared Spectroscopy (FTIR, Bruker Tensor 37) was recorded in the range 600-4000 cm⁻¹ range with a resolution of 4 cm⁻¹ to observe the changes in functional groups.

2.3.1 FESEM Characterization:

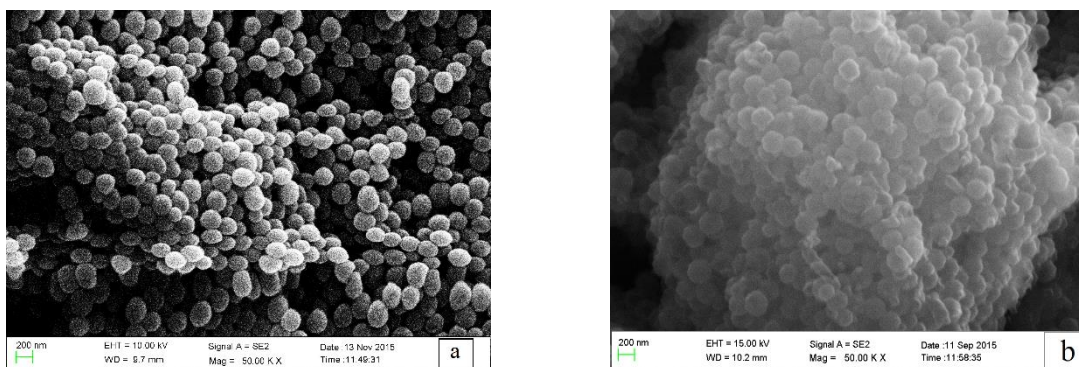


Figure2: FESEM images of a) PVDF Powder & b) CDI-1400

Fig. 2a and 2b shows the FESEM images of PVDF powder before and after pyrolysis at 1400°C respectively. From the image can clearly observe that morphology of the nanoparticles is intact after pyrolysis. The particle size before pyrolysis is observed to be ~290nm which remained unchanged even after pyrolysis.

2.3.2 HRTEM Characterization:

TEM images (Figure 3) clearly reveals that particle size is 290 nm and each spherical particle, the disordered areas consists of smaller crystallites randomly arranged of graphene is clearly observed in the pyrolyzed sample. From this, we can conclude that carbon derived from PVDF precursor is a hard carbon. This disordered carbon shows high capacity because of more surface area accessible to intercalation of Li ions due to the pores formed between disoriented graphene layers which facilitate more surface area for Li-ions to intercalate [16].

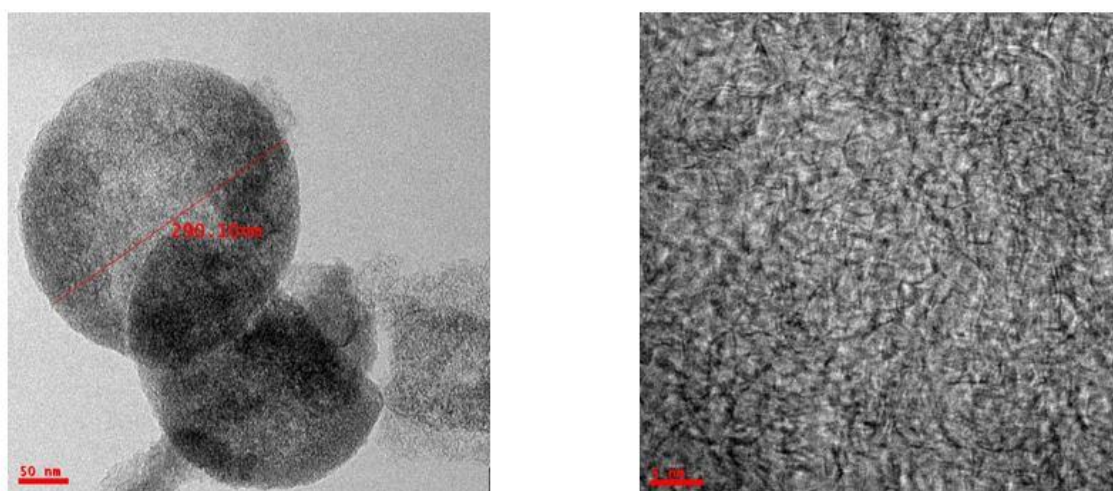


Figure 3: HRTEM images of CDI-1400 at different magnifications

2.3.3 FTIR Analysis:

The chemical functionalities of samples were investigated using FTIR spectrum as shown in fig. 4. C-F stretching vibration corresponds to the peak at 1180 cm^{-1} [14] which can be seen in all the samples. We can observe the decrease in peak intensity when compared PVDF powder fig.4a with dehydrofluorinated sample (PDI) fig.4b which indicates fluorine content is reduced in the sample by dehydrofluorination reaction to some extent. The indication of dehydrofluorination reaction is the formation of conjugated double bonds between carbon,

decrease in intensity of characteristic peaks from 1400 cm^{-1} to 500 cm^{-1} [14] and formation of hydroxyl functional groups [15].

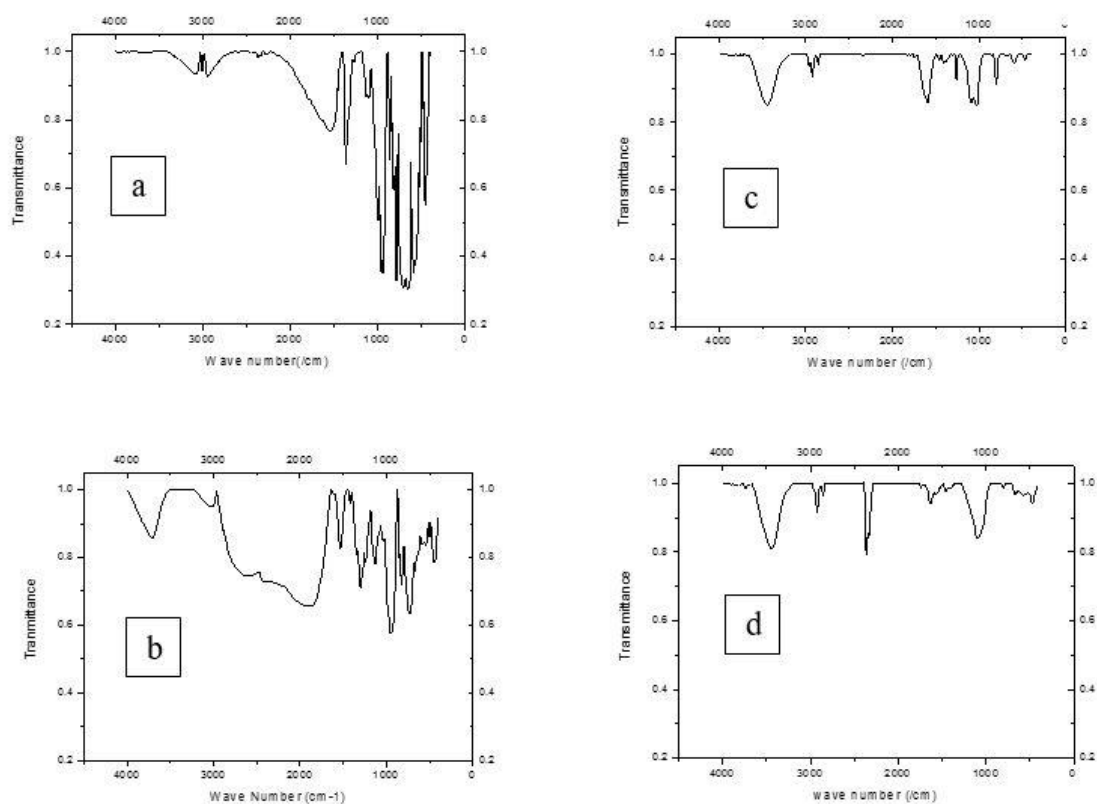


Figure 4: Comparison of FTIR spectrum of a) PVDF; b) PDI; c) CDI-900; d) CDI-1400

Effect of carbonization on the removal of these functional group is studied at three different temperatures (900°C , 1200°C , and 1400°C). We can observe with an increase in carbonization temperature the intensity of C-F (1180 cm^{-1}) peak decreases which indicates a decrease in fluorine content. At the same time, we can observe the increase in the intensity of C-C triple bond (2260 cm^{-1} - 2100 cm^{-1}) in fig 4d.

2.3.4 Characterization by XRD:

X-ray diffraction studies have been conducted for all carbonized samples. The broad peaks of (0 0 2) & (1 0 1) in patterns from the fig.5b and fig.5c show typical hard carbon which is amorphous in nature [17]. The characteristic peak at 38° in fig.5a is due to NaF, which is formed during dehydrofluorination reaction [18]. It is observed that increase in pyrolysis temperature

from 900°C to 1200°C, could decompose the NaF which is formed in dehydrofluorination reaction.

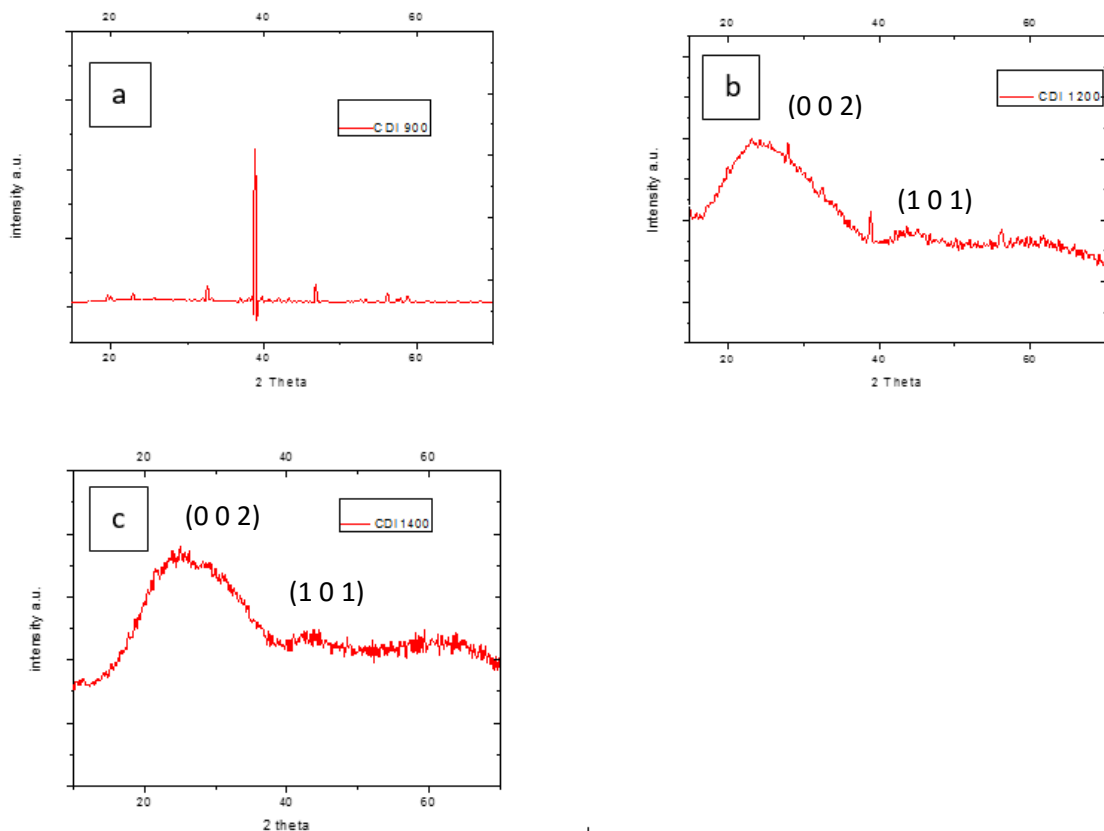


Figure 5: XRD plots of carbon derived at different temperatures a) CDI 900; b) CDI 1200 and c) CDI 1400

From this XRD peaks analysis, we can conclude that the carbon derived from PVDF at 1200°C and 1400°C is a typical hard carbon where graphene layers are highly disoriented which is evident in HRTEM fig.3.

2.4 Electrochemical Performance of CDI X samples

2.4.1 Galvanostatic Charge/discharge Cycling at 0.1 C Rate

For all the given samples, the capacity is due to a combination of intercalation and disorder mechanism. From Figure 6, we observe that the CDI 1400 exhibited higher reversible capacity (297 mAh/g) than the other two samples (CDI 900 and CDI 1200) after 11 cycles of charge

discharge at 0.1 C rate. The coulombic efficiency was found to be more than 94 % after 11 cycles for all three samples. A detailed analysis of electrochemical performance is summarised in Table 1.

| Sample | First cycle | | | After 11 cycles | |
|----------|-----------------------------|-------------------------------|-------------------------|-----------------------------|-------------------------|
| | Reversible Capacity (mAh/g) | Irreversible Capacity (mAh/g) | Columbic efficiency (%) | Reversible Capacity (mAh/g) | Columbic efficiency (%) |
| CDI-900 | 12 | 83 | 12.4 | 8 | 89 |
| CDI-1200 | 83 | 279 | 23 | 61 | 96 |
| CDI-1400 | 478 | 1030 | 30 | 297 | 94.6 |

TABLE 1: Summary of specific capacities of CDI samples pyrolyzed at different Temperatures at 0.1 C- rate

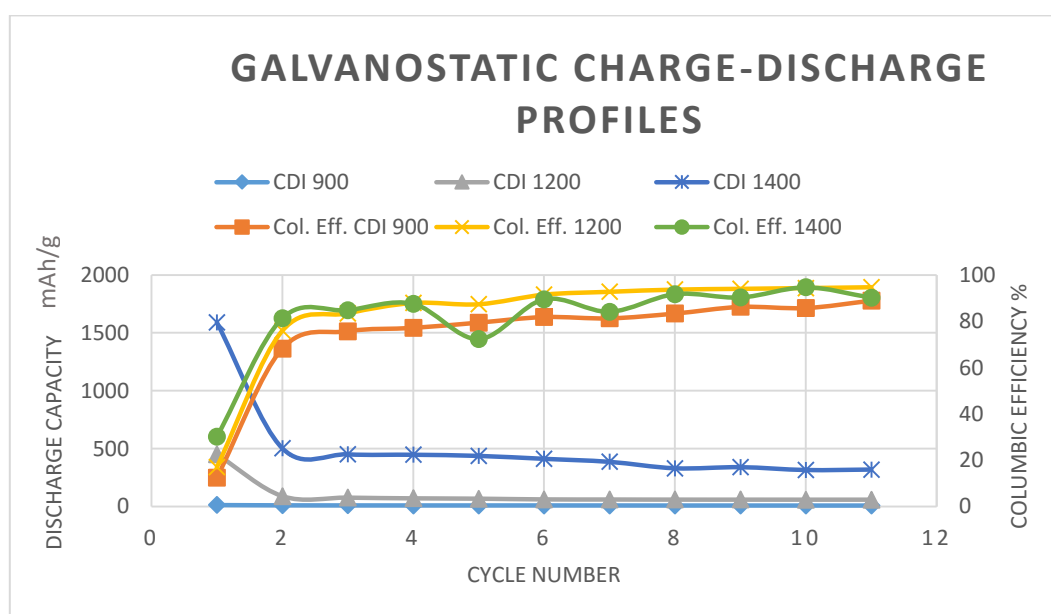


Figure 6: Comparison of cycling behaviour at 0.1 C rate for carbonized samples for different temperatures.

Yield of Carbon at different temperatures:

| S.no | Sample | Yield |
|------|----------|---------|
| 1 | CDX-900 | 70 % |
| 2 | CDX-1200 | 50.4 % |
| 3 | CDX-1400 | 30.66 % |

TABLE 2: Summary of yields of carbon obtained after pyrolysis

From the table 1 first cycle reversible capacity (~ 478 mAh/g) and coulombic efficiency (~30%) was significantly higher for CDI 1400. Regardless formation of solid electrolyte interface will lead to a loss of lithium ions in few cycles resulting high irreversible capacity. However, the reversible capacity is stabilised at 297 mAh/gm with 94.7% columbic efficiency. This excellent electrochemical behaviour of CDI X samples can be well explained by their structural characteristics.

From XRD and TEM studies, we observed that all CDI X samples are amorphous in nature. Significantly the contribution to the capacity is due to intercalation mechanism. At the surface, Lithium reacts with carbon and electrolyte which results in the formation of the passive layer [19]. Because of its high surface area for hard carbons, the irreversible capacity will also be high. Capacity fade in this sample could be attributed to its high porosity. If a sample is porous in nature, then electrolyte accumulates in the pores which serve as a reaction site for the Li-ions to react and thus continuously form a passive layer [20]. Whenever Li-ions are trapped inside the pores [21], there will be an irreversible loss of Li-ions.

From Table 2, we also report a high yield of carbon by adding dehydrofluorination step before pyrolysis (~70%) which is significantly higher than reported value in T Zheng et. al [15]. It is observed that yield decreased with increase in pyrolysis temperature as additional functional groups start decomposing at higher temperatures.

2.4.2 Cyclic Voltammetry:

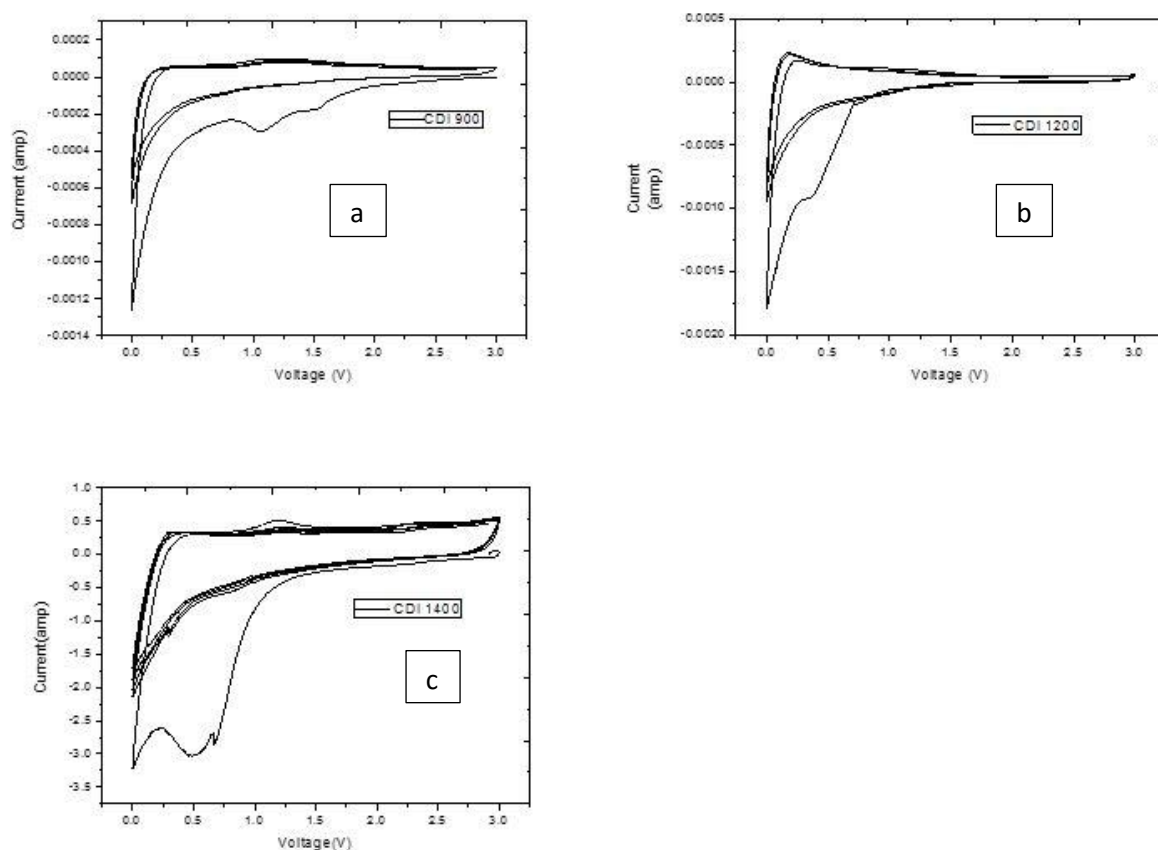


Figure 7: Cyclic voltammetry study for (a) CDI 900; (b) CDI 1200; and (c) CDI 1400

The cyclic voltammograms are shown in fig. 7 were recorded at 1mV/s between 0 and 3 volts. High current in discharge state of the cell is because of passive layer formation which is due to decomposition of the electrolyte with lithium ions on the anode surface. The current peak at 0.6V in the first cycle of all samples shows the formation of the passive layer. The peak at 0.1V is due to deintercalation of Li ions from carbon [22]. In fig 7c, the hysteresis between charge and discharge is too high as it is suffering from high irreversible capacity.

2.5 Conclusion:

Hence, we have improved the yield of carbon from PVDF by adding dehydrofluorination step before pyrolysis. From the structural analysis, we can conclude that the carbon obtained is a hard carbon which showed significantly higher capacity. Higher capacity with excellent columbic efficiency makes PVDF as one of the best precursors for carbon. Further improvement in capacity is envisaged with catalytic graphitization.

Chapter 3

3D Carbon Fractal Structures as Anode for Li-ion Batteries

3.1 Introduction:

Carbonaceous materials have a lot of potential applications in various fields because of its existence in different crystalline forms [23-24]. Recently, microfabrication of carbonaceous materials has received attention because its various applications in miniaturisation of energy storage devices. Photolithography is one of the techniques for fabrication of MEMS. In this method, Photoresist is used as base material where exposure to UV radiation can change its properties. By having photoresist as starting material, we can achieve low resolutions with repeatability.

The photoresist is light sensitive material where its properties like viscosity, adhesion and solubility can be altered with exposure time and baking temperatures. There are two kinds of Photoresists, i.e., positive tone photoresist and negative tone photoresist. SU 8 is one the most well-known epoxy-based negative tone photoresists. Negative tone refers to a photoresist where the parts which are exposed to UV will be cross-linked while the unexposed areas of the film remain soluble and can be washed away during development using developer. In 1996 MicroChem was the first to introduce SU-8 products commercially. It is a viscous polymer which can be spun to give a broad range of thicknesses from 2 μ m to 300 μ m on a single coat [26].

Typically, a well-polished doped Silicon wafer is used as a substrate for this MEMS devices fabrication. It shows excellent adhesion property towards SU-8 photoresist which enables us to fabricate High Aspect Ratio Structures, but it is having high resistivity (0.001 ohm-cm) as well. Usually, Stainless steel wafer is used as a current collector in Li-ion batteries. So to explore the full potential of SU 8 as a precursor for carbon as an anode, we patterned the

microstructures on Stainless steel wafer which is a better conductor than silicon. Then we pyrolyze the sample using two step pyrolysis procedure to get carbon out of patterned structures [27]. Madou et. al. used silicon as substrate and fabricated micro carbon posts that could be intercalated reversibly with Li ions [27-28].

In the current study, we have fabricated the SU-8 derived carbon micropillars 3D on SS wafer by utilising C-MEMS process. These micropillars on S.S. wafer, acts as an anode for our Li-ion battery. The process conditions were finely tuned to control the peeling of carbon microstructures during pyrolysis from the wafer. SU-8 microstructures were pyrolyzed at 900°C on S.S. wafer. Thus prepared 3D carbon microstructures on SS wafer were then characterised by optical profiler for aspect ratio analysis before and after pyrolysis. Prepared carbon microelectrodes were tested for electrochemical performance with 0.1C rate, and results were reported.

3.2 Materials and methods:

Materials:

SU-8 2150, 2050, 2010 from (Microchem Corp., MA), SS substrates from (MTI Corp, USA) and lithium foil (99.9% pure, Sigma-Aldrich). Glass microfibre filters (Whatman) and LP-30 electrolyte (1M solution of LiPF₆ in a 1:1 v/v mixture of ethylene carbonate and diethyl carbonate) from Merck were used as received.

Methods:

Polished Stainless Steel wafer is taken, and SU-8 (Microchem Corp., MA) of our choice was spin-coated in a yellow room at 3000 rpm for 30 s on SS substrate (MTI Corp., USA). Thus obtained thin film was prebaked on a hot plate at 65°C and 95°C for optimised timings to remove the excess solvent from the film. Now the film is exposed to UV radiation through the mask of desired patterned. Then Post bakes the sample at 65°C and 95°C to enhance reaction rate which promotes crosslinking. Develop the patterned film with SU 8 developer (Microchem Corp., MA) to wash away unexposed parts. Then the formed SU 8 microstructures were hard baked at 150 for 5mins to release the internal stresses developed during the crosslinking. Hard baked samples were then pyrolyzed at 900°C to obtain carbon microstructures.

Schematic of C-MEMS

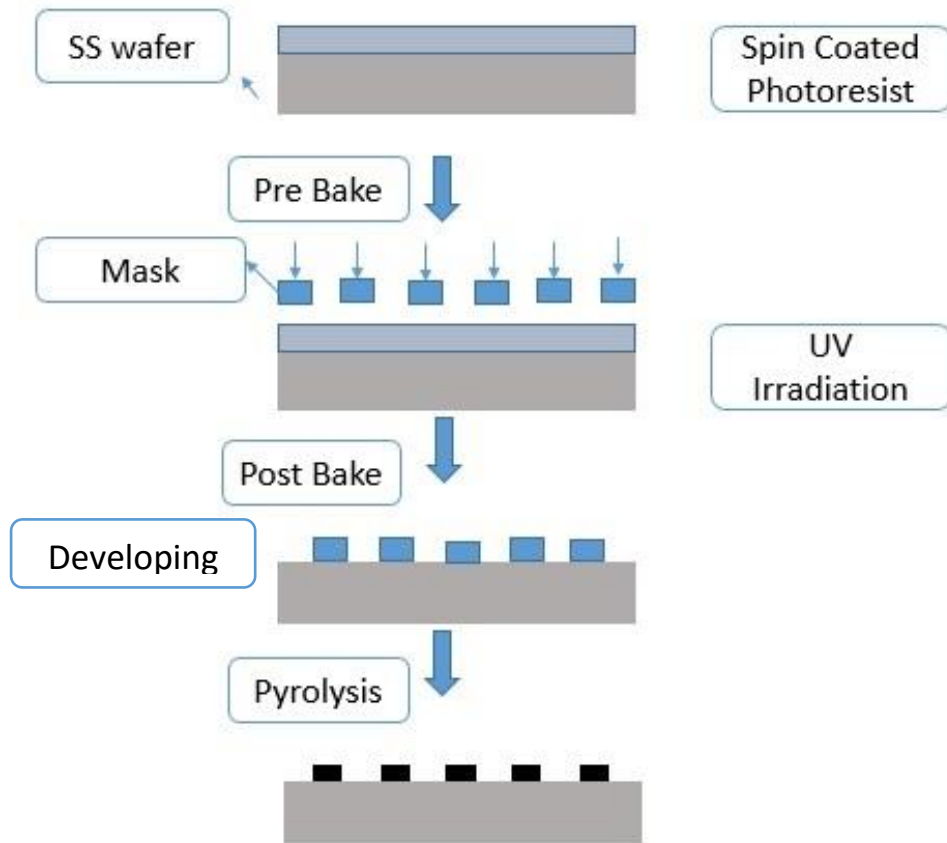


Figure 8: Schematic of C-MEMS

3.2.1 Fabrication of different aspect ratios Fabrication:

After running, numerous experiments we have come up with the optimised experimental conditions for fabricating various Aspect ratio (height/width) for micropillars on S.S. substrate. Using single and multiple coats we were able to fabricate the micropillars with a height range of 50-500 micrometres. The details of fabricated samples information are given in Table 3. Prepared samples were analysed using 3D Optical Profiler and Scanning Electron Microscope for finding out height and width. The motivation behind this fabrication of different aspect ratios microstructures is to study the effect of height and width on electrochemical performances of the anode.

Table 3: Summary of micropillars fabricated with different Aspect ratios.

| S. No | Material | Coat | Height μm | Width μm | Aspect Ratio |
|-------|------------------------|----------|--------------|-------------|-----------------|
| 1 | SU-8 2050 | Single | 51 | 150 | 0.33 |
| 2 | SU8- 2100 | Single | 110 | 172 | 0.63 |
| 3 | SU8-2150 | Single | 220 | 170 | 1.3 |
| 4 | SU8-2150 + SU8-2010 | Multiple | 381 | 154 | 2.47 |
| 5 | SU8-2150 + SU8-2010 | Multiple | 514 | 240 | 2.14 |

Steps involved in Fabrication 514μm height structures with aspect ratio 2.14(Sample 5)

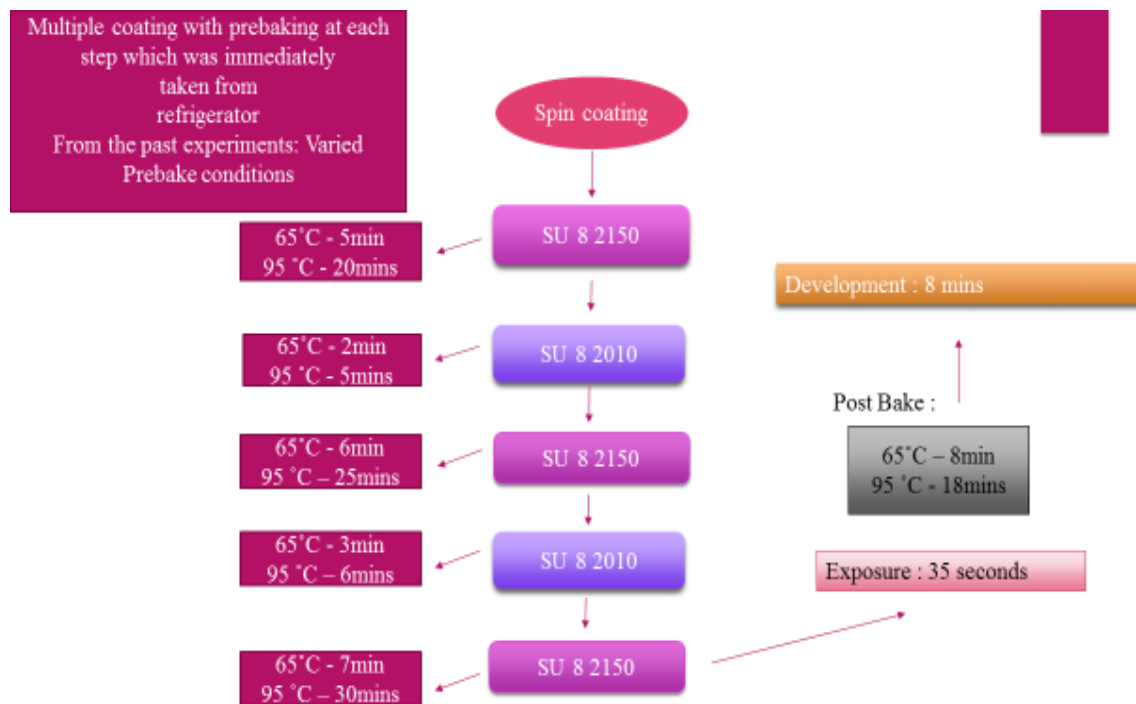


Figure 9: Schematic of Fabrication process of sample 5 in the above table

3.2.2 Pyrolysis:

As-prepared SU-8 microstructures were then carbonised at 900°C in the inert atmosphere using two-step pyrolysis in an alumina tube furnace (Nabertherm GmbH). Samples were introduced into the furnace at room temperature. The furnace tube was initially purged with 100 lph N₂ flow for 20 min. After initial purging, the Nitrogen flow rate was maintained constant at 50 lph to remove the dissolved oxygen in SU 8 during decomposition. The temperature of the furnace was ramped up to 350 °C at 2°C /min, and samples were kept at the same temperature for 30 min. These samples were further ramped up at 5°C /min to 900 °C and held at 900°C for 1 hour before cooling to room temperature in the presence of the inert gas atmosphere.

3.2.3 Electrode Preparation:

The prepared SU-8 derived-carbon structures on SS wafers were then used as working electrodes and tested for their electrochemical performance using a Galvanostat potentiostat (Biologic Potentiostat, Model: VSP). Lithium foil (99.9% pure, Sigma-Aldrich) was used as a counter electrode in a Swagelok cell assembly. 1 M solution of LiPF₆ in a 1:1 v/v mixture of ethylene carbonate and diethyl carbonate was used as an electrolyte while glass microfiber filters (Whatman Filters) were used as a separator. The Swagelok cell assembly was completely packed inside an argon-filled glove box with trace amounts of moisture and oxygen. The soaking time was maintained for 12 hours before Galvanostatic cycling at a C-rate=C/10 to measure the Li-ion intercalation capacity of SU-8 derived-carbon structures as an anode.

3.3 Characterization

3.3.1 SEM characterization

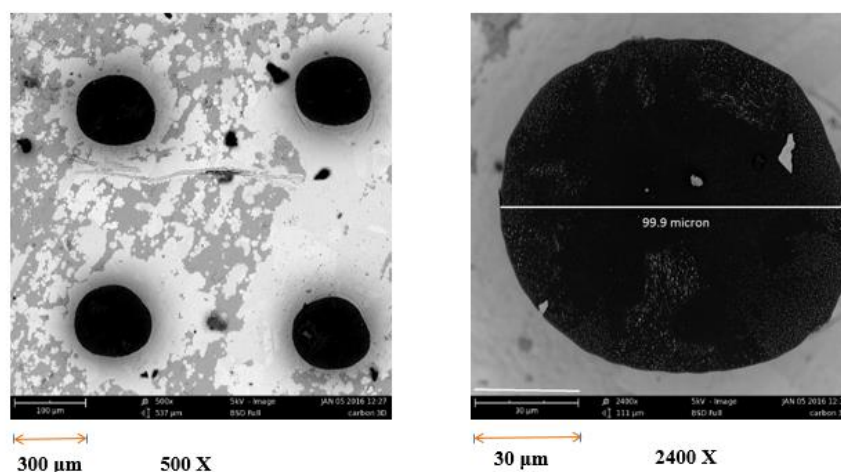


Figure 10: SEM images of SU 8 derived carbon micropillars

The SEM image is Carbon micropillars of 100microns diameter,100microns and 200 micron spacing are obtained from pyrolysis of sample 3 SU 8(220-microns height and 170-microns width 120-microns spacing) in Table 3. The aspect ratio decreased from 1.3 to 1 after pyrolysis which shows that shrinkage is anisotropic. The yield of carbon that we obtained was 25% after pyrolysis Rest of the SU 8 decomposed during the pyrolysis process.

3.3.2 Optical Profiler analysis:

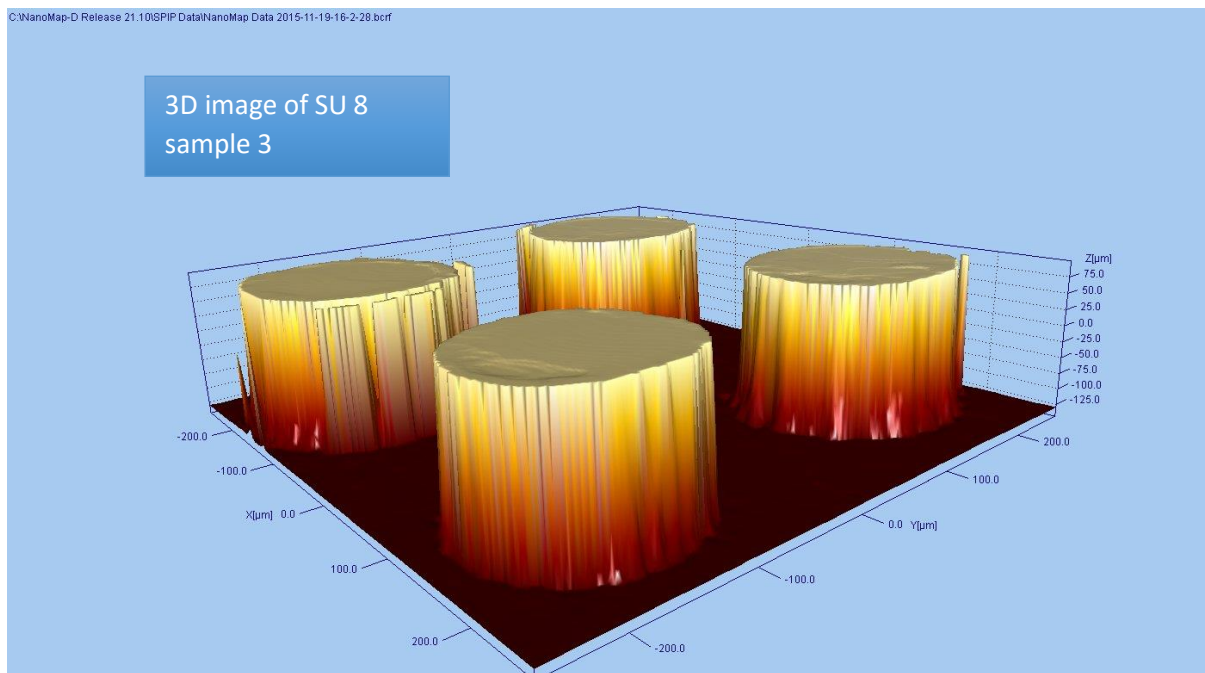
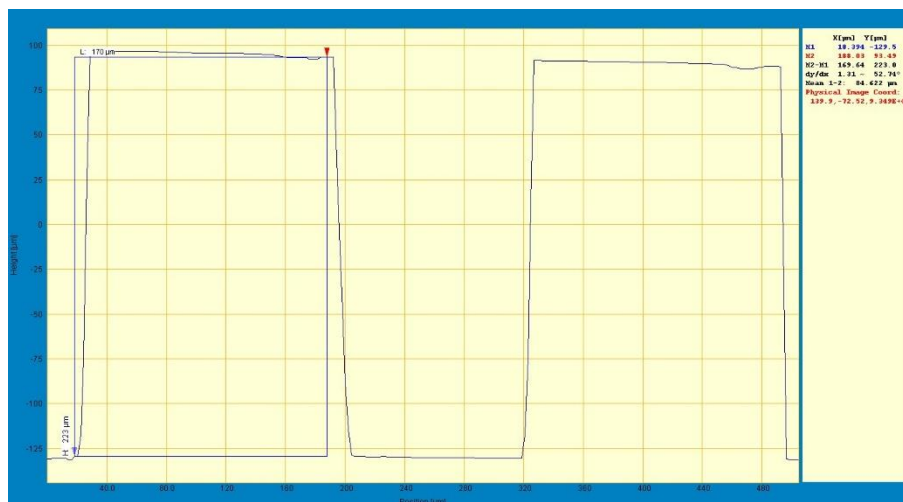


Figure 11: 3D image of SU 8 micropillars of sample 3



Height: ~220 μm
Width: ~170 μm
Aspect Ratio: 1.3

Figure 12: 2D image of SU 8 micropillars of sample 3

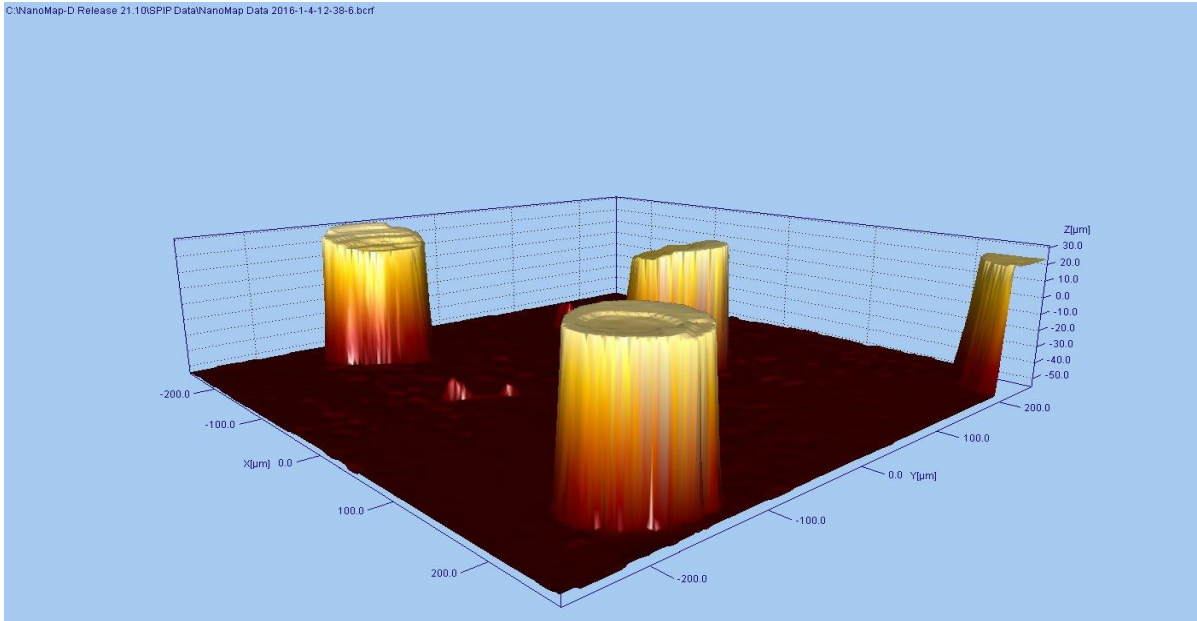
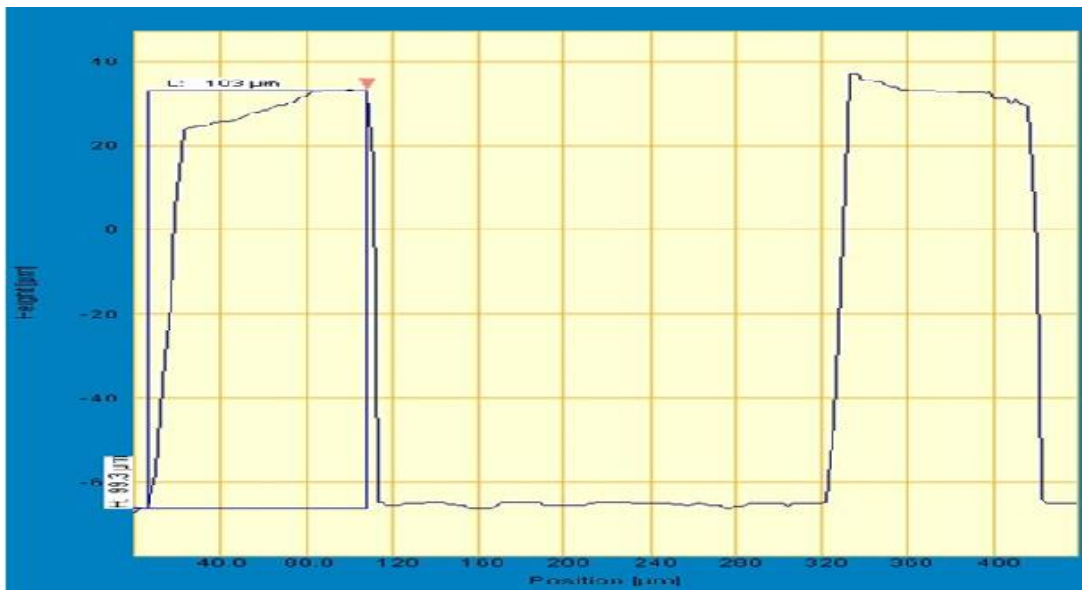


Figure 13: 3D image of SU 8 derived carbon micropillars of sample 3



Height: ~100 μm Width: ~100 μm Aspect Ratio: 1

Figure 14: 2D image of SU 8 derived carbon micropillars of sample 3

The above images are of Carbon micropillars (fig.6&7) of 100microns, and 100microns are obtained from pyrolysis of sample 3 SU 8(220-microns height and 170-microns width) fig.5 in Table 3. The aspect ratio decreased from 1.3 to 1 after pyrolysis which shows that shrinkage is anisotropic. This is evident from the 3D Optical Profiler images.

3.4 Electrochemical Performance:

3.4.1 Galvanostatic Charge/Discharge at 0.1C rate:

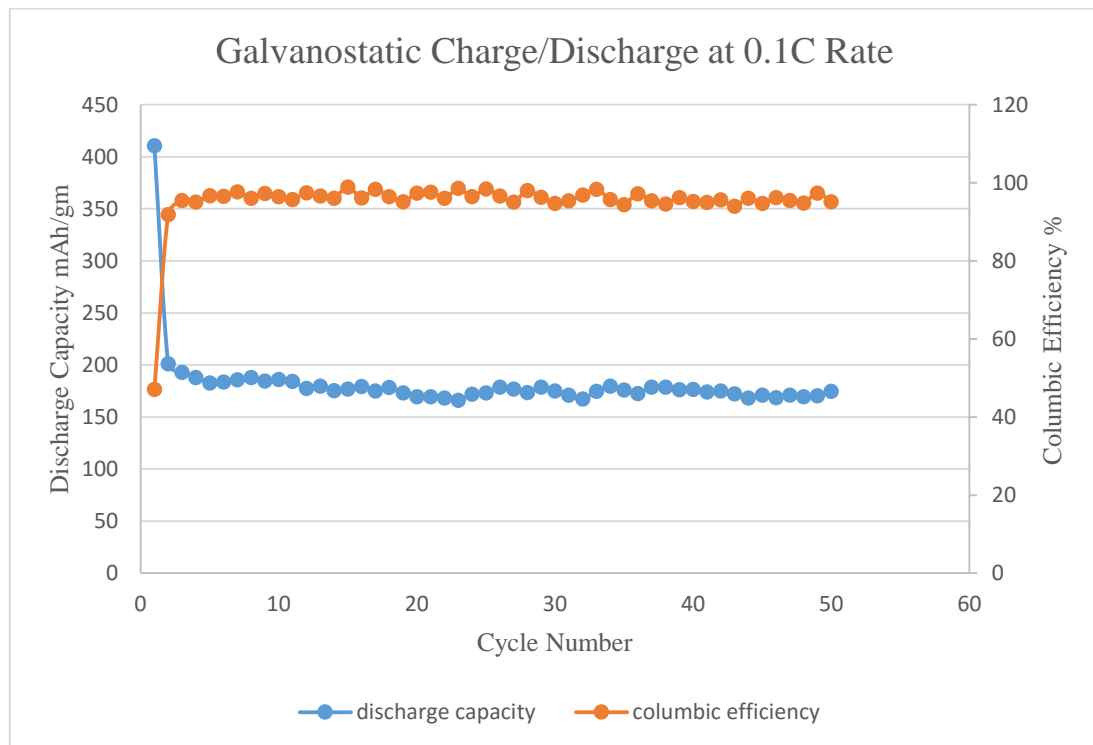


Figure 15: Galvanostatic Charge/Discharge of microelectrode at 0.1C Rate

From the fig.15, it is evident that the first cycle discharge capacity is 410 mAh/gm (graphite=372mAh/gm) with columbic efficiency 47% at 0.1C rate. Because of the formation of a passive layer on anode which consumes Li-ions irreversibly, the first cycle efficiency is low. After 50 cycles of charge-discharge, the discharge capacity faded to 171.99mAh/gm and charge capacity to 161.2 mAh/gm.

3.5 Summary:

An epoxy-based negative photoresist (SU-8) derived-carbon structures were successfully prepared on SS wafer used as substrates and then further tested for their electrochemical performance as anode materials for Li-ion battery. Galvanostatic charge/discharge experiments

showed higher discharge capacity (~410 mAh/g) in the first cycle as compared to that for graphite and earlier reported values, and showed improved coulombic efficiency. Higher capacity with enhanced coulombic efficiency makes SU-8 photoresist-derived carbon structures on SS wafers a better alternative for anode materials in Li-ion batteries. Further deposition of Candle soot or SU 8 microfibers on these carbon structures may be useful to achieve the high energy density architecture further for Lithium-ion batteries.

Chapter-4

Summary and Future Directions

4.1 Summary

In this thesis, we have reported the electrochemical performances of hard carbons derived from PVDF and SU 8. In Chapter 2, we studied the capacity dependence on pyrolysis temperature and observed how structural changes lead to the improvement of capacity. We also report a high yield of carbon by adding dehydrofluorination step before pyrolysis (~70%) which is significantly higher than reported value. From the structural analysis, we can conclude that the carbon obtained is a hard carbon which showed considerably higher capacity. Higher capacity with excellent columbic efficiency makes PVDF as one of the best precursors for carbon.

In chapter 3, we reported electrochemical performance of Carbon microelectrode on SS wafer. We optimised the experimental conditions for different aspect ratios of stable micropillars on SS wafer. We successfully pyrolyzed the SU 8 micropillars to get carbon microelectrode which can act as an anode in Li-ion battery. Using SEM and 3D optical profiler, the analysis for aspect ratios were examined before and after pyrolysis.

4.1.1 Fine tuning of hard carbon

In the second chapter, we have reported the significant increase in capacity by increasing the pyrolysis temperature. It helped us to eliminate Functional groups attached which is confirmed by FTIR analysis. We have increased the yield of carbon by adding dehydrofluorination step which removes fluorine partially. In preparing carbon microelectrode, we were constrained with 900 °C pyrolysis temperature to study its effect on electrochemical performance. Beyond 900 °C the SS wafer will start bending, so no attempts were made to change the crystallinity by varying pyrolysis temperature.

4.1.2 Characterization

Various characterization studied the chemical composition and hard carbon microstructure. In chapter 2, with the help of FESEM we were able to observe whether the samples were contaminated or not with the support of EDX. HRTEM characterization provided information about the disordered regions. It also supported XRD results by revealing the disorientation of Graphene layers in hard carbon. FITR analysis helped us to confirm the functional groups in the samples. It contributed to us confirm the removal of Fluorine during dehydrofluorination and carbonisation. In Chapter 3, Using 3D Optical Profiler we analysed the aspect ratios of micropillars which were further confirmed by SEM analysis.

4.1.3 Electrochemical performance

In Chapter 2, the sample which was pyrolysed at the highest temperature in the studies showed the better performance. We could eliminate the fluorine functional groups to the extent of 20%. CDI-1400 is tested at high C-Rates as well, but the performance is low. The samples further showed a high recovery capacity when reverted back to low C-rate. This suggests structure to be stable and suitable for Low C-rate application. Thus, we were able to demonstrate the potential of PVDF derived carbon as an anode for Li-ion battery.

In Chapter 3, The Electrochemical performance results of carbon microelectrode suggest the High Aspect Ratio Structures (>4) as we can have more surface area than our present samples. Thus we were able to report a new substrate (SS wafer) for C-MEMS process.

4.2 Future Directions

- i) The primary challenge impeding the usage of hard carbons is the capacity fade observed which was even found in the CDI samples as well as graphitised specimens. If we could address the issue by doing some chemical treatment or by synthesizing composites, it would be vital in further enhancing the hard carbon usage for both high and low C rate applications.
- ii) We can go Catalytic Graphitization of PDI samples to get ordered graphene regions which enhance the cyclability.
- iii) PVDF can be electrospun and cast as a film as well. So by Nano Structuring, we can further change the morphology and improve its electrochemical performance further.

- iv) For the First time, we have reported C-MEMS fabrication on Stainless Steel Substrate. To improve electrochemical performance of the microelectrode, we can decrease the distance between the pillars and increase the Aspect ratio to get more Surface area for Li-ion intercalation.
- v) Depositing SU 8 derived carbon fibers and beads on this microelectrode can further enhance the surface area which helps to improve capacity.
- vi) The carbon derived from SU 8 is hard carbon which is showing better performance at low C-Rates. Our group has reported candle soot as potential anode material for High C-Rates applications. So, we can combine these two materials by just depositing candle soot on the carbon micropillars to get an enhanced surface area for candle soot. It can improve electrochemical performance.

THE END

References

- [1] T. P. Kumar, T. S. D. Kumari, and A. M. Stephan. Carbonaceous anode materials for lithium-ion batteries - the road ahead. *J Indian Inst Sci* 89, (2009) 393–424.
- [2] M. B. Pinson and M. Z. Bazant. Theory of SEI formation in rechargeable Batteries: capacity fade, accelerated aging and lifetime Prediction. *J Electrochem.Soc* 160, (2013) A243–A250.
- [3] D. S. Su and R. Schlogl. Nanostructured carbon and carbon nanocomposites for electrochemical energy storage applications. *ChemSusChem* 3, (2010) 136–168.
- [4] J-M. Tarascon and G. G. Amatucci. *Microengineering aerospace systems*. 1st edition. The Aerospace Press, 1999.
- [5] Z. Ogumi and M. Inaba. *Advances in lithium ion batteries*. 1st edition. Kluwer Academic Publishers, 2002.
- [6] Y. Liu, J. S. Xue, T. Zheng, and J. R. Dahn. Mechanism of lithium insertion in hard carbons prepared by pyrolysis of epoxy resins. *Carbon* 34, (1996.) 193–200.
- [7] M. Kakunuri, S. Vennamalla, and C. S. Sharma. Synthesis of carbon xerogel nanoparticles by inverse emulsion polymerization of resorcinol formaldehyde and their use as anode materials for lithium-ion battery. *RSC Adv* 5, (2015) 4747–4753.
- [8] V. Agubra and J. Fergus. Lithium ion battery anode aging mechanisms. *Materials* 6, (2013) 1310–1325.
- [9] Y. P. Wu, E. Rahm, and R. Holze. Effects of heteroatoms on electrochemical performance of electrode materials for lithium ion batteries. *Electrochim. Acta* 47, (2002) 3491–3507.

- [10] W. Lu and D. D. L. Chung. Effect of the pitch-based carbon anode on the capacity loss of lithium-ion secondary battery. *Carbon* 41, (2003) 945–950.
- [11] Doron Aurbach, Ella Zinigrad, A short review of failure mechanisms of lithium metal and lithiated graphite anodes in liquid electrolyte solutions. *Solid State Ionics* 148 (2002) 405 – 416
- [12] M Endo, C Kim Recent development of carbon materials for Li ion batteries. *Carbon* Volume 38, Issue 2, 2000, Pages 183–197.
- [13] T. Zheng, Y. Liu, E. W. Fuller, S. Tseng, U. Von Sacken, and J. R. Dahn. Lithium insertion in high capacity carbonaceous materials. *J. Electrochem. Soc* 142, (1995) 2581–2590.
- [14] H.Kiese and H.Ogata. Phase transfer catalysis in dehydrofluorination of poly(vinylidene fluoride) by aqueous sodium hydroxide solutions. *J. Polym. Sci., Part A: Polym. Chem.* 21, (1983) 3443-3451.
- [15] J. Wootthikanokkhan and P. Changsuwan. Dehydrofluorination of PVDF and proton conductivity of the modified PVDF / sulfonated SEBS blend membranes. *J. Metals, Mater. Miner.*18, (2008) 57–62.
- [16] E. Buiel et. al./ *Electrochimica Acta* 45 12-130 (1999).
- [17] Aleksandra P. Kierzek K. Properties and Lithium insertion behaviour of hard carbons produced by pyrolysis of various polymers at 1000°C. *Journal of Analytical and Applied Pyrolysis* Volume 102, July 2013 Pages 1-6
- [18] L. Leal-Curz et. al. A. Zojomo. (ISSN 1833-122) Volume 5 (2009)
- [19] Pallavi Verma, Pascal Maire, A review of the features and analyses of solid electrolyte interphase in Li-ion Batteries. *Electrochimica Acta.* 55(2010) 6332-6341.

- [20] V. Agubra and Jeffrey Fergus. Lithium Ion battery anode aging mechanisms. *Materials* 2013. 6(4), 1310-1325.
- [21] K.Guerin, M.Menetrier A.Fevrier-Bouvier, Li NMR study of a hard carbon for lithium – ion rechargeable batteries. *Solid State Ionics* 127, (2000) 187–198.
- [22] H. Kataoka, Y. Saito, O. Omae, J. Suzuki, K.Sekine,T.Kawamura and T.Takamura. Lithium storage mechanism of disordered mesophase carbon fibers studied by Li-NMR. *Electrochem. Solid-State Lett* 5, (2002) 10-13.
- [23] K. P. De Jong and J. W. Geus, “Carbon nanofibers: Catalytic synthesis and applications,” *Catalysis Rev.-Sci. Eng.*, vol. 42, pp. 481–510, 2000.
- [24] T. Edmonds, “Electroanalytical applications of carbon-fiber electrodes,” *Anal. Chimica Acta.*, vol. 175, pp. 1–22, 1985.
- [25] Lorenz H *et al* 1998 High-aspect-ratio, ultrathick, negative-tone near-UV photoresist and its applications for MEMS *Sensors Actuators A* **64** 33–9.
- [26] C.Wang, G. Jia, L. H. Taherabadi and M. J. Madou, *J. MEMS*, 14(2), 348 (2005).
- [27] G. T. Teixidor, R. B. Zaouk, B. Y. Park and M. Madou, *J. Power Sources*, 183, 730 (2008)

